1   **Individual differences in time-varying and stationary brain connectivity during movie watching**

2   **from childhood to early adulthood: Effects of age, sex, and behavioral associations**

3

4   Xin Di[1*], Ting Xu[2], Lucina Q. Uddin[3], Bharat B. Biswal[1*]

5

6   1. Department of Biomedical Engineering, New Jersey Institute of Technology, Newark, NJ 07102, USA

7   2. Center for the Developing Brain, Child Mind Institute, New York, NY 10022, USA

8   3. Department of Psychiatry and Biobehavioral Sciences, University of California at Los Angeles, Los

9   Angeles, CA 90095, USA

10

11

12   * Corresponding author:

13   Xin Di, Ph.D.

14   604 Fenster Hall, University Height

15   Newark, NJ, 07102, USA

16   xin.di@njit.edu

17

18   Bharat B. Biswal, Ph.D.

19   607 Fenster Hall, University Height

20   Newark, NJ, 07102, USA

21   bbiswal@yahoo.com

22

23   **Running title:** Individual differences in connectivity

24

25 **Abstract**

26 Spatially remote brain regions show dynamic functional interactions during various task conditions.

27 Time-varying functional connectivity measured during movie watching was sensitive to movie content,

28 while stationary functional connectivity remains stable across videos. Therefore, it has been suggested

29 that dynamic and stationary functional interactions may reflect different aspects of brain function.

30 However, how individual differences in time-varying and stationary connectivity are associated with

31 behavioral phenotypes is still unclear. We analyzed an open-access functional MRI dataset collected from

32 participants (5 to 22 years old) as they watched two cartoon movie clips. Regional brain activity, time-

33 varying and stationary functional connectivity were calculated, and associations with age, sex, and

34 behavioral assessments were examined. Using a model comparison method, we showed that time-varying

35 connectivity was more sensitive to age and sex effects compared with stationary connectivity. The

36 preferred age models were quadratic log age or quadratic age effects, corresponding to inverted-U shaped

37 developmental curves. In addition, females showed higher consistency in regional brain activity and time-

38 varying connectivity than males. However, in terms of behavioral predictions, only stationary

39 connectivity could predict full-scale intelligence quotient. The results suggest that individual differences

40 in time-varying and stationary connectivity may reflect different aspects of behavioral phenotypes.

41

42 **Keywords**: brain connectivity, brain development, model comparison, movie watching, time-varying

43 connectivity.

44

1. Introduction

45

46   Functional integration between spatially remote brain regions is thought to be critical to understanding

47   brain functions. Functional connectivity is characterized by the statistical dependency between observed

48   brain signals (Friston, 1994). This stationary characterization of functional connectivity can be studied

49   during the resting-state (Biswal et al., 1995, 2010), and has furthered our understanding of brain

50   functional organization (Biswal et al., 2010; Margulies et al., 2016; Yeo et al., 2011). On the other hand,

51   functional connectivity is also highly dynamic (Allen et al., 2014). Whole-brain dynamic connectivity

52   patterns constitutes different "states" (Allen et al., 2014), which are reliable (Abrol et al., 2017).

53   Disruptions to dynamic connectivity have been associated with varies mental disorders (Fu et al., 2019).

54   In recent years, movie watching has emerged as an alternative paradigm between the

55   unconstrained resting-state and well controlled task experiments. Participants' experience when watching

56   video clips is more "natural" than performing some cognitive tasks. In addition, movie watching bears

57   advantages over resting-state in terms of scanning compliance and with potentially lower head motion

58   artifacts (Vanderwal et al., 2019). When watching the same movie clip, different participants tend to show

59   similar patterns of brain activity (Hasson et al., 2004), which could be taken as an indicator of functional

60   significance of the observed brain activity. Time-varying connectivity also shows high constancy across

61   participants (Di et al., 2022; Di and Biswal, 2020), which supports the functional significance of time-

62   varying measures of functional connectivity.

63   Time-varying and stationary functional connectivity may reflect distinct aspects of brain function.

64   Many studies have found that the stationary connectivity during watching of different movies is very

65   similar (Di et al., 2022; O'Connor et al., 2017; Tian et al., 2021), and may even be highly correlated with

66   other mental states, such as resting-state (O'Connor et al., 2017). On the other hand, time-varying

67   connectivity can depend on the movie content, thus dynamic patterns and region pairs involved have been

68   shown to vary greatly between different movie clips (Di et al., 2022). This seems to suggest that the time-

69   varying connectivity may be more sensitive to reflect moment-to-moment brain function. More generally,

70   during resting-state, time-varying connectivity can capture unique behavioral variability compared with

71 stationary connectivity (Eichenbaum et al., 2021). A handful studies on disease classifications showed

72 that resting-state time-varying connectivity has better predictive power than stationary connectivity to

73 classify schizophrenia, bipolar disorder (Rashid et al., 2016), and post-traumatic stress disorder (Jin et al.,

74 2017).

75   To further explore the functional relevance of time-varying and stationary connectivity, we aim to

76 examine individual differences in time-varying and stationary connectivity during movie watching. Age

77 and biological sex are common factors that give rise to individual variations. When watching movie clips,

78 adults showed higher synchronized regional activity compared with children (Cantlon and Li, 2013;

79 Petroni et al., 2018), but children may show distinct patterns of responses compared with adults (Di and

80 Biswal, 2022). A few studies have examined age effects on time-varying and stationary connectivity in

81 the resting-state (Faghiri et al., 2018; Marusak et al., 2017; Rashid et al., 2018). They found linear

82 correlations between some dynamic connectivity measures and age. In the current study, we utilized more

83 complex age models and a model comparison framework to examine age effects. We asked whether time-

84 varying and stationary connectivity differently represent age and sex effects.

85   Further, we ask whether individual differences in time-varying and stationary connectivity are

86 associated with behavioral outcome measures. In the resting-state, time-varying connectivity performed

87 better than stationary connectivity in predicting behavioral phenotypes (Eichenbaum et al., 2021) and in

88 classification of mental disorders (Jin et al., 2017; Rashid et al., 2016), and post-traumatic stress disorder

89 (Jin et al., 2017). Therefore, it is reasonable to expect that the time-varying connectivity during movie

90 watching may also perform better than stationary connectivity in predicting behavioral outcome measures.

91   In the current study, we analyzed movie watching fMRI data from a large open-access dataset

92 called the Healthy Brain Network (HBN) (Alexander et al., 2017). A few studies have utilized this dataset

93 to examine model-based brain activations (Richardson, 2019), stationary connectivity (Vanderwal et al.,

94 2021), and event segmentation (Cohen et al., 2022) during the movie watching. Female and male

95 participants age between 5 to 22 years were recruited in this project, with rich behavioral assessments and

96 MRI scanning. From the fMRI data during movie watching, we calculated regional activity, stationary

97   connectivity, and time-varying connectivity. We used a model comparison framework to examine the age

98   and sex effects on the different brain measures, and adopted a predictive modeling approach to examine

99   the prediction power of these brain measures on behavioral measures. We hypothesize that time-varying

100   connectivity will show stronger evidence of age and sex effects compared with stationary connectivity

101   and regional activity, and time-varying connectivity will also show higher prediction power than

102   stationary connectivity and regional activity in predicting behavioral outcomes.

103

104   **2. Materials and Methods**

105   **2.1. Healthy Brain Network dataset**

106   **2.1.1. Dataset and participants**

107   The MRI data were obtained from the Healthy Brain Network project website

108   (http://fcon_1000.projects.nitrc.org/indi/cmi_healthy_brain_network/) (Alexander et al., 2017). We

109   identified 279 participants who have no diagnosis of any psychiatric or neurological disorders and have

110   T1 weighted MRI data available (up to Release 9). We performed stringent quality control on the T1

111   weighted structural images and fMRI images (see below for details). 159 participants' structural images

112   were found with motion artifacts or lesions. After additionally removing participants with excessive head

113   motion during fMRI scans (maximal framewise displacement smaller than one voxel), 87 participants for

114   'The Present' dataset and 83 participants for the 'Despicable Me' dataset were included in the current

115   analysis. Among them, 66 participants overlapped. For all the included participants, there were 61 males

116   and 43 females (age range 5.0 to 21.9 years, *Mean = 12.0*; *Standard Deviation = 4.1*).

117   **2.1.2. MRI data**

118   We analyzed fMRI data collected while the participants watched two animated movie clips. The first is a

119   short film 'The Present' (3 minutes and 21 seconds long, Filmakademie Baden-Wuerttemberg, 2014). The

120   second is a 10-minute clip from the animated film 'Despicable Me' (Illumination, 2010). The high-

121   resolution anatomical MRI images were also used for preprocessing purposes.

122   MRI data were acquired from two MRI centers, Rutgers University Brain Imaging Center

123   (RUBIC), with a 3T Siemens Trio scanner, and Citigroup Biomedical Imaging Center (CBIC), with a 3T

124   Siemens Prisma scanner. The scanning protocols were similar across sites. For fMRI, the key imaging

125   parameters were as follows: TR = 800 ms; TE = 30 ms; flip angle, 31°; voxel size = 2.4 x 2.4 x 2.4 mm^{3};

126   multi-band acceleration factor = 6. For T1 weighted anatomical MRI, the images were acquired using

127   either the Human Connectome Project (HCP) or the Adolescent Brain Cognitive Development (ABCD)

128   sequences. The sequences are different in terms of voxel sizes, however, the anatomical images were only

129   used for preprocessing of the fMRI images. For more information about the MRI protocols, please refer to

130   the HBN project website and (Alexander et al., 2017).

131   **2.1.3. Behavioral measures**

132   We picked two behavioral measures, full-scale intelligence quotient (FSIQ) from the Wechsler

133   Intelligence Scale for Children – Fifth Edition (Wechsler, 2014) and the Social Communication

134   Questionnaire (SCQ) (Rutter et al., 2003). FSIQ measures general cognitive ability, which is widely used

135   in studies of brain-behavior relationships (Vieira et al., 2022). 64 and 60 participants with the video clip

136   'The Present' and with the clip 'Despicable Me' had FSIQ scores available, respectively. SCQ is a parent

137   report questionnaire that measures social and communication symptoms related to autism spectrum

138   disorder. In a previous work using the same dataset, it has been reported that the SCQ scores were

139   associated with brain activation during certain time points (events) (Richardson, 2019). 70 and 65

140   participants with the video clip 'The Present' and the clip 'Despicable Me' had SCQ scores available,

141   respectively.

142   **2.2. MRI data processing**

143   **2.2.1. Structural MRI quality control and processing**

144   We visually inspect the MRI images for all the participants. Issues noted included excessive head motion,

145   partial coverage, or brain lesions. We performed visual quality control on the T1 weighted images as well

146   as segmented images. 159 participants' images were found with ghost artifacts, motion artifacts, or

147   lesions. MRI data of 120 participants were included in the current analysis.

148　　　　　Statistical parametric mapping (SPM12, https://www.fil.ion.ucl.ac.uk/spm/) in MATLAB

149　　(R2021a, https://www.mathworks.com/) was used for MRI image processing. The T1 weighted image for

150　　each participant was first segmented into gray matter, white matter, cerebrospinal fluid, and other tissue

151　　types, and roughly aligned into standard Montreal Neurological Institute (MNI) space using linear

152　　transformation. Then the DARTEL procedure was used to register the segmented gray matter and white

153　　images across all the individuals and generate a sample specific template through several rounds of

154　　iterations (Ashburner, 2007). The averaged gray matter template was then linearly normalized to MNI

155　　space.

156　　**2.2.2. Functional images preprocessing**

157　　Functional images were realigned to the first image, coregistered to the anatomical image, and then

158　　normalized into MNI space. During the normalization step, the functional images were resampled into 2.4

159　　x 2.4 x 2.4 mm^3 voxel size, and spatially smoothed using an 8 mm Gaussian kernel. Lastly, voxel-wise

160　　general linear model (GLM) was used to remove head motion artifacts and low-frequency drifts. The

161　　GLM included Friston's 24 head motion parameters (Friston et al., 1996), and 1/128 Hz high pass filter.

162　　The residual images from the GLM step were used for further analysis.

163　　　　　Head motion is considered an important factor that affects BOLD fMRI signals. We removed

164　　participants who's maximum framewise displacement in any directions or movie clips were larger than

165　　2.4 mm or 2.4^o (proximately the size of a voxel). Next, we examined the association of head motion and

166　　the observed age effects. First, we showed that the frame-wise displacement time series were not

167　　synchronized across subjects. The first PC explained less than 5% of variance (Figure S1A). Secondly, we

168　　used mean frame-wise displacements in translation and rotation as measures of head motion, and

169　　examined their age effects. Model comparison showed that for 'The Present' clip, a constant model

170　　without age effects was favorable (Figure S1C and S1D). However, for the 'Despicable Me' clip, there

171　　was evidence of log age effects (Figure S1E and S1F). The age effect patterns on head motion look very

172　　different from the age effects on the brain measures. Nevertheless, we added mean framewise

173　　displacement of translation and rotation in the age fitting models.

7

2.2.4. Independent component analysis

We first utilized independent component analysis (ICA) to reduce the dimensionality of the fMRI data (Di et al., 2022; Di and Biswal, 2022). The ICA was performed using the Group ICA Of fMRI Toolbox(GIFT) (Calhoun et al., 2001) with data from both video clips combined together. Twenty independent components (ICs) were extracted and visually inspected. Eighteen components were considered functional meaningful networks. Based on our previous work (Di et al., 2022; Di and Biswal, 2022). Four networks are specifically of interest due their involvement in movie watching (Di et al., 2022; Di and Biswal, 2022): the dorsal visual network, temporoparietal junction, supramarginal network, and the default mode network (particularly the posterior cingulate cortex) (Figure 1A). The time series for each of the 18 networks were back reconstructed for each participant and video clip, which were used for further analysis.

2.3. Statistical analysis

2.3.1. Regional activity and connectivity measures

Inter-subject correlation has been used to index shared responses during movie watching (Hasson et al., 2004; Nastase et al., 2019). Here we used a principal component analysis (PCA) based method to estimate inter-individual consistency (Di and Biswal, 2022). For each network (IC), the time series from each participant formed a t x n matrix, where t and n represent the number of time points and participants, respectively. The matrices were 250 x 87 for the clip 'The Present', and 750 x 83 for the clip 'Despicable Me'. We performed PCA on the matrix, and obtained the variances explained by the first and second PCs. A circular time-shift randomization method was used to determine the null distribution with 10,000 times randomizations (Di and Biswal, 2022; Kauppi et al., 2010). The loadings of the first PC were used as a measure of individual differences.

Between each pair of two networks (ICs), we calculated point-by-point interactions (multiplications) to index time-varying connectivity (Di et al., 2022; Faskowitz et al., 2020). We similarly performed PCA to estimate the inter-individual consistency of the time-varying connectivity. The loadings of the first PC were used as an index of individual differences in time-varying connectivity.

8

200   Lastly, we calculated stationary connectivity as the Pearson's correlation of the time series

201   between each pair of the 18 networks (ICs).

202   **2.3.2. Age and sex effects**

203   We adopted a model comparison framework to examine age and sex effects on regional activity,

204   stationary connectivity, and time-varying connectivity. For each region or region pair of a brain measure,

205   we built five models of age effects, with sex as a separate regressor. Additional covariates included a

206   scanner site variable and mean framewise displacement in translation and rotation. The five models are as

207   follows,

208     $$y = \beta_0 + \beta_1 \cdot sex + \beta_2 \cdot site + \beta_3 \cdot FD_{Trans} + \beta_4 \cdot FD_{Rot} + \varepsilon \quad (1)$$

209     $$y = \beta_0 + \beta_1 \cdot age + \beta_2 \cdot sex + \beta_3 \cdot site + \beta_4 \cdot FD_{Trans} + \beta_5 \cdot FD_{Rot} + \varepsilon \quad (2)$$

210     $$y = \beta_0 + \beta_1 \cdot age + \beta_2 \cdot age^2 + \beta_3 \cdot sex + \beta_4 \cdot site + \beta_5 \cdot FD_{Trans} + \beta_6 \cdot FD_{Rot} + \varepsilon \quad (3)$$

211     $$y = \beta_0 + \beta_1 \cdot \log(age) + \beta_2 \cdot sex + \beta_3 \cdot site + \beta_4 \cdot FD_{Trans} + \beta_5 \cdot FD_{Rot} + \varepsilon \quad (4)$$

212     $$y = \beta_0 + \beta_1 \cdot \log(age) + \beta_2 \cdot \log(age)^2 + \beta_3 \cdot sex + \beta_4 \cdot site + \beta_5 \cdot FD_{Trans} + \beta_6 \cdot FD_{Rot} + \varepsilon \quad (5)$$

213   Where y represents a specific measure such as regional activity in a network, stationary connectivity, or

214   time-varying connectivity between two networks. Model 1 represents a baseline condition where there is

215   no age effect. Models 2 and 3 represent linear age effect and quadratic age effect models. Models 4 and 5

216   represent log age effect and quadratic log age effect models. The log age models consider the fact that

217   brain measures may grow faster and then decrease slower within the studied age range. We additionally

218   built five models the same as models 1 through 5 except that there were no sex effects in each of the

219   models. Therefore, we had 10 models in total (2 x 5).

220   To compare different age models and sex effects, we used a model comparison procedure. The 10

221   models were fitted with the ordinary least square method, and the Akaike information criterion (AIC) was

222   calculated. We then calculated Akaike weights (Wagenmakers and Farrell, 2004) for each model. Akaike

223   weights quantify the model evidence of a specific model relative to the best model among all the 10

224   models, with the sum of all the models as 1. We first asked what age model best to describe the

9

225   developmental effects. The Akaike weights of the same age model with and without the sex term were

226   added as the model evidence of a particular age effect, regardless of the sex effects (Portet, 2020).

227   Similarly, for the sex effect, we added the Akaike weights for all five age models with the sex term. The

228   sums of model weights depend on the number of alternative models. We adopt a threshold of 0.6 for the

229   age model comparison (5 models) and 0.8 for the sex effect comparison (2 models).

230   **2.3.3. Behavioral prediction analysis**

231   We applied ridge regression to study brain-behavioral associations. The predicted variable was either

232   FSIQ scores or SCQ scores, which was an *n* by *1* vector. *N* were different for FSIQ and SCQ scores and

233   for the two movie clips due to data availability. The predicting variables were either regional activity,

234   stationary connectivity, or time-varying connectivity. We applied a leave-one-out cross-validation to

235   evaluate the prediction value for each brain measure. Specifically, we held out one participant's data, and

236   used the remaining *n – 1* data to obtain a prediction model. We used a linear model for the prediction.

$$y = \beta_0 + X \cdot \beta + \varepsilon$$

237   where *y* is a *n – 1* vector of either FSIQ of SCQ scores, *X* is a *n – 1* by *m* matrix of regional activity,

238   stationary connectivity, or time-varying connectivity matrices. For the regional activity, *m* equals to 18 of

239   the networks. For the matrices, the number of column equals *153* (*18 x 17 / 2*), which is larger than the

240   number of rows. We used a dimension reduction procedure to keep 18 features to match with the number

241   of regional activity. To do so, all the features were correlated with the predicted variable, and the first 18

242   features with the highest absolute correlations were kept. Therefore, *X* is always a *n – 1* by *18* matrix. The

243   model was fitted with a ridge regularization. The regularization parameter λ was determined using a

244   nested cross-validation procedure for each training set. Using the optimal λ, the model was trained using

245   the *n – 1* training data. The model was applied to the held-out participant to calculate the predicted value.

246   The procedure was performed *n* times for the *n* participants, resulting in *n* predicted values. We calculated

247   the correlation between the predicted value and the actual values across all n participants to obtain an

248   estimate of prediction accuracy.

249   The optimal λ was determined for each leave-one-out sample using an inner leave-one-out loop.

250   Within the $n - 1$ outer-loop training set, we built linear models with $n - 2$ individuals with 21 λ values

251   (from 2^{-10} to 2^{0} in logarithmical space). The prediction accuracies across all the inner loop samples were

252   calculated for all the λ values. The λ with the highest correlation was parsed to the outer loop as the

253   optimal λ for model training and prediction. The prediction procedure is outlined in Supplementary Figure

254   S1.

255   To evaluate the prediction accuracies, we used the correlation coefficient between the predicted

256   and observed values. There are in total 12 predictions (2 movies x 3 brain measures x 2 behavioral

257   measures). We used false discovery rate correction to account for multiple comparisons ($q < 0.05$).

258

259   **3. Results**

260   **3.1. Regional activity**

261   We first focused on the inter-individual consistency and differences in regional activity when watching

262   the two video clips. We performed PCA on the time point by participant matrices of regional activity in

263   each of the 18 included networks (ICs). The first PCs in all the 18 networks explained a statistically

264   significant amount of variance for both videos. However, none of the second PCs explained significant

265   variance. Therefore, we focused on the first PCs in the following analysis. Figure 1B shows the

266   percentage variance explained by the first PC in the 18 networks for the two movie clips. In addition to

267   lower-level sensory networks such as the visual and auditory networks, a few higher-level networks also

268   showed high inter-individual consistency, including the dorsal visual network (IC3), temporoparietal

269   junction network (IC4), supramarginal network (IC7), and default mode network (IC16). There are also

270   noticeable differences between the two video clips. In particular, a network covering the posterior insula,

271   secondary somatosensory regions and cingulate (IC9) showed more than 2 fold in variance explained by

272   the first PC in 'The Present' (23.0%) than 'Despicable Me' (10.0%). We submitted the map to

273   Neurosynth for cognitive decoding (Yarkoni et al., 2011). After removing terms related to brain labels,

274   the top five terms were pain, painful, tactile, stimulation, and touch.

11
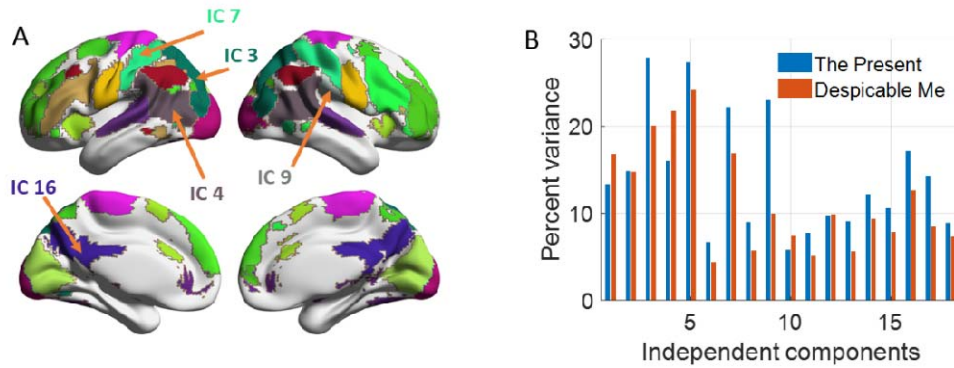
Figure 1 A, Maps of eighteen independent components that were included in the current analysis. The maps were thresholded at z > 3 after z transformations of the original IC maps, and were shown in a winner-take-all manner when overlapping. The arrows indicate the networks of interest for movie watching, IC3, dorsal visual; IC4, temporoparietal junction; IC7 supramarginal; IC9, secondary somatosensory; and IC16, posterior cingulate. BrainNet Viewer was used for visualization (Xia et al., 2013). B, inter-individual consistency of regional activity (percent variance explained by the first principal component) for the two video clips.

We then applied a model comparison procedure to examine the age and sex effects. Figure 2A and 2B shows the model evidence among the five age models for the 18 network ICs and the two video clips. For the networks with a strong preference of a model, the preferred model was usually the quadratic log age or quadratic age model. We identified the network ICs where a specific age model had model evidence higher than 0.6, and plotted the fitted effects in Figure 2D and 2F. All the age effects showed an inverted-U shape, with peak loadings around 10 years of age. The quadratic log age models indicated a faster increase in the younger age and slower decrease in older age. Figure 2E and 2G further show individual loadings as well as the fitted curves for the two curves on the top of Figure 2D and 2F. Figure 2E corresponds to the supramarginal network (IC7) in the video clips of 'The Present', and Figure 2G corresponds to the bilateral parietal junction network (IC4) in the 'Despicable Me' clip.

12
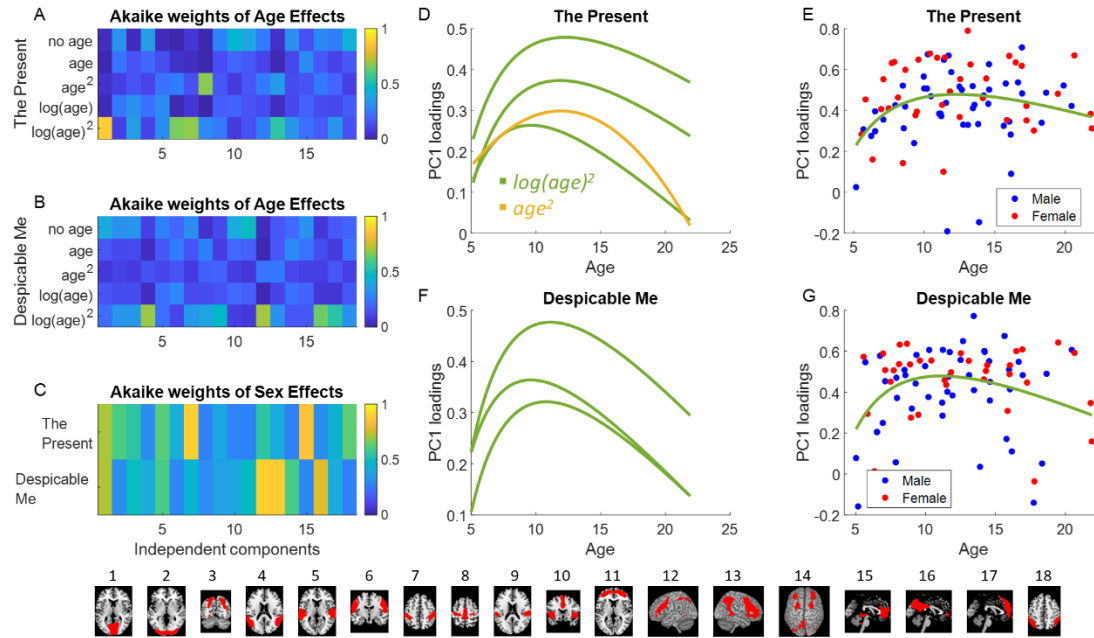
Figure 2 Model comparison results for different age models for regional activity in the 18 network independent components (ICs) for the video clips The Present (A) and Despicable Me (B). C shows the model evidence of the sex effects. D and F show fitted effects of the ICs who had Akaike weights of one model over 0.6. E and G show the PC1 loadings of two representative ICs as functions of age, which correspond to the top curves in D and F, respectively.

Four networks showed strong evidence of a sex effect (> 0.8) on regional activity for the two video clips differently (Figure 2C). For 'The Present', the supramarginal network (IC7) (model probability = *88.36%*) and medial frontal network (IC15) (model probability = *85.76%*) showed evidence of sex effects. While for the video clip of 'Despicable Me', the left (IC12) and right (IC13) fronto-parietal networks showed evidence of sex effects (model probability = *88.80%* and *87.50%*, respectively). For all the effects, the females showed higher consistency than the males.

3.2. Stationary connectivity

13

309   The group averaged stationary connectivity matrices for the two video clips are shown in Figure 3A and

310   3E. The two matrices were similar, which is in line with our previous work (Di et al., 2022). Higher

311   stationary connectivity was observed mainly between networks with similar functions, e.g., among visual

312   networks and among fronto-parietal networks.
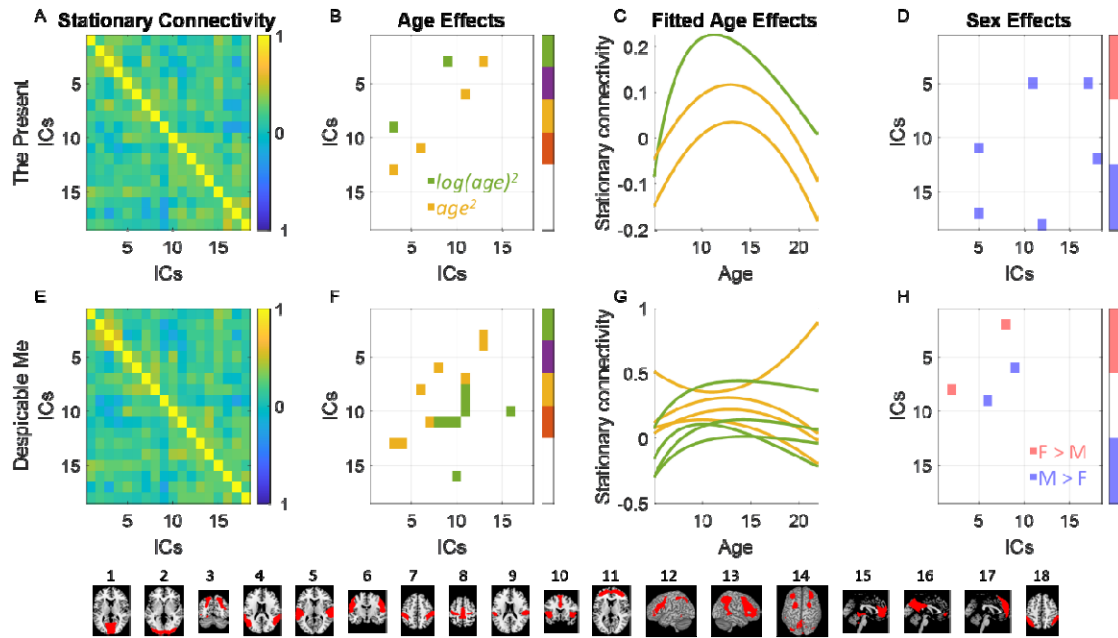
313

314   **Figure 3** A and E, group averaged stationary connectivity among 18 independent component (IC)

315   networks for the two video clips. B and F, connectivity with winning age models with model evidence

316   greater than 0.6. C and G, fitted curves with corresponding color representing the specific age models. D

317   and H, connectivity with evidence of sex effects greater than 0.8. The bottom row shows the

318   representative maps of the 18 networks.

319

320   The model comparison results for the age and sex effects on the stationery are shown in

321   Supplementary Figure S3. The connections that showed preferences of an age model with greater than 0.6

322   model evidence are shown in Figure 3B and 3F. The preferred age models were either quadratic log age

323   or quadratic age models. All but one age effects showed an inverted-U shapes (Figure 3C and 3G). Three

324   connections showed a preference of an age model for the clip of 'The Present', and eight connections

325   showed a preference of an age model for the 'Despicable Me' video. One stationary connectivity during

14

326 'The Present' involved two networks of interest, i.e., the dorsal visual network (IC3) and secondary

327 somatosensory network (IC9). And the patterns of age effects appeared to be quite different for the two

328 video clips. In addition, three connections for the clip of 'The Present' and two connections for the

329 'Despicable Me' clip showed sex effects, but they were not among the networks of interests related to

330 movie watching.

331

332 **3.3. Time-varying connectivity**

333 Figure 4A and 4E show the consistency of time-varying connectivity for the two movie clips. In general,

334 the clips of 'The Present' showed higher consistency of time-varying connectivity. Interestingly, the time-

335 varying connectivity among many networks of interest, i.e., the dorsal visual network (IC3),

336 supramarginal network (IC7), and secondary somatosensory network (IC9) showed high consistency.

337 Moreover, the medial prefrontal network (IC17), which is part of the default mode network, also showed

338 consistent time-varying connectivity with the other regions of interest.
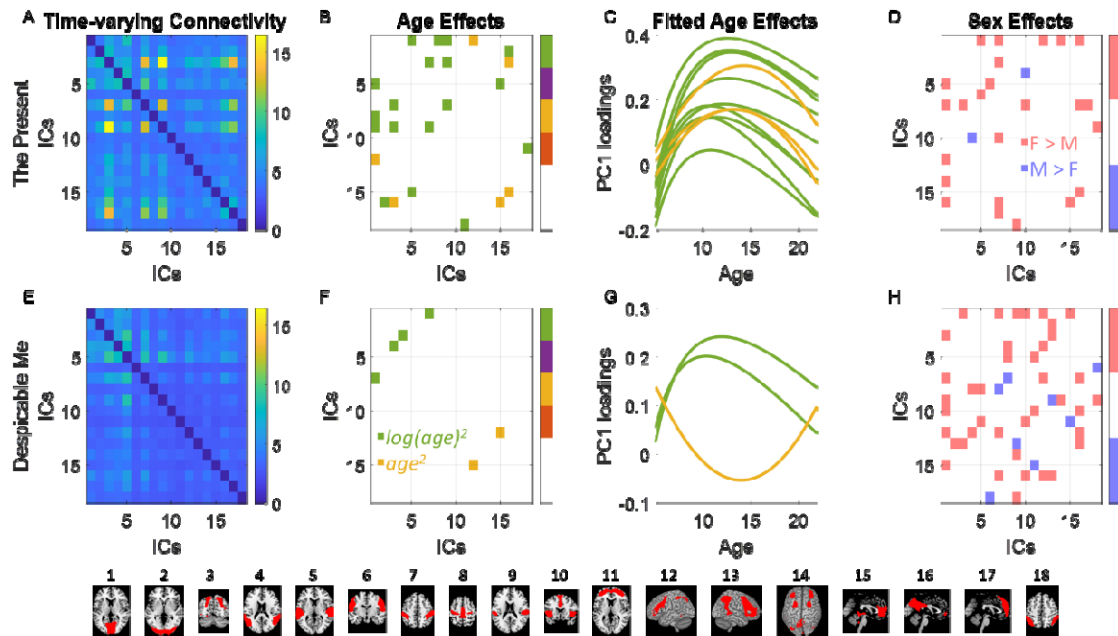
339

340 **Figure 4** A and E, the inter-individual consistency of time-varying connectivity (percent variance

341 explained by the first principal component) among 18 networks (independent components, ICs) for the

342 two video clips. B and F, connectivity with winning age models with model evidence greater than 0.6. C

15

343   and G, fitted curves with corresponding color representing the specific age models. D and H, connectivity

344   with evidence of sex effects greater than 0.8. The bottom row shows the representative maps of the 18

345   networks.

346

347   The age effects on time-varying connectivity also preferred quadratic log age or quadratic age

348   effects (Supplementary Figure S3 and Figure 4B and 4F). Fourteen connections showed strong

349   preferences to an age model for the video 'The Present'. Interestingly, time-varying connectivity among

350   the dorsal visual (IC3), supramarginal (IC7), and secondary somatosensory (IC9) networks strongly

351   preferred the quadratic log age effects. In contrast, only three connections showed strong preferences to

352   an age model for the video 'Despicable Me'.

353   Many connections also showed strong evidence of sex effects, mainly with higher consistency in

354   females than males (Figure 4D and 4H). This included time-varying connectivity between the dorsal

355   visual (IC3) and the supramarginal networks (IC7).

356

357   **3.4. Behavioral relevance**

358   Lastly, we used machine learning regression to examine the behavioral relevance of regional activity,

359   stationary connectivity, and time-varying connectivity. Two behavioral measures were studied: FSIQ and

360   SCQ scores. With leave-one-out cross-validation, we estimated the prediction accuracy of the three types

361   of brain measures on FSIQ and SCQ scores. Only stationary connectivity showed statistically significant

362   prediction accuracies (Figure 5). Using stationary connectivity from both video clips, we could predict

363   FSIQ scores with accuracies of around 0.35. Individual differences of regional activity and time-varying

364   connectivity could not predict FSIQ scores (Supplementary Figure S5). In addition, none of the brain

365   measures could predict SCQ scores (Supplementary Figure S6).
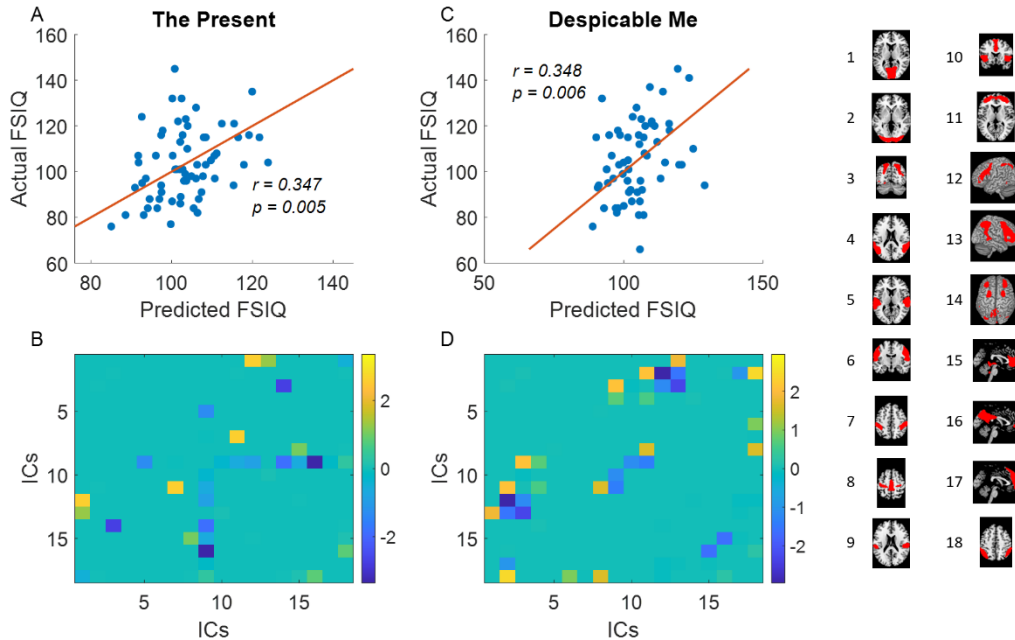
Figure 5 Results of full-scale intelligence quotient (FSIQ) predictions using stationary connectivity for the two video clips. Top row, each dot represents a predicted value using leave-one-out cross validation and its corresponding actual value. The red line indicates $y = x$. Bottom row, averaged weights of the prediction model across all the LOO models. The maps of the corresponding independent components (ICs) are shown on the right.

4. Discussion

In the current study, we examined individual differences in stationery and time-varying connectivity, as well as regional activity, during movie watching in a sample of children to young adults. Consistent with our hypothesis, time-varying connectivity was more sensitive to age and sex effects compared with stationary connectivity and regional activity. In contrast to our hypothesis, however, only stationary connectivity could predict FSIQ scores.

The two animated video clips evoked consistent brain activations across individuals in higher order brain regions, including the dorsal visual, temporoparietal junction, supramarginal, and the default

17

382   mode networks, which have shown similar consistent responses with different movie clips and samples

383   (Di et al., 2022; Di and Biswal, 2022). Many of these regions, e.g., the temporoparietal junction,

384   supramarginal, and default mode networks are involve in processing of higher order social information, as

385   might be expected during watching of the movie clips. More interestingly, a unique independent

386   component covering the secondary somatosensory cortex, posterior insula, and cingulate cortex showed

387   much higher consistency in the clip of 'The Present' compared with the clip of 'Despicable Me'. These

388   regions are related to higher somatosensory and pain process, and may be involved in empathy for pain

389   (Allen et al., 2017; Lamm et al., 2007). Because 'The Present' involves a scene of an amputated limb, it is

390   reasonable that these regions are involved. Our discussions will focus on these networks.

391   For all the connectivity and activity measures, the optimal age models were quadratic log-age or

392   age effects, mostly exhibiting an inverted-U shape. Time-varying and stationary connectivity showed age

393   effects in different connections, with time-varying connectivity showing age effects between regions

394   related to movie watching. The inverted-U shape indicates that the brain measures increase during early

395   childhood and later decrease toward adulthood. This provides a more complete picture of synchronized

396   responses compared with previous studies with only two groups of adults and children (Cantlon and Li,

397   2013; Petroni et al., 2018). The reduced synchrony in adults compared with teen age children may

398   indicate that neural processing is more efficient in adults therefore requiring less activation. Alternatively,

399   the adult participants may have more idiosyncratic responses to the video clips, or the cartoon nature may

400   make the adult participants less engaged in watching them. Nevertheless, a practical implication is that

401   when controlling for age effects, a simple linear model may not be sufficient.

402   We observed widespread sex effects for time-varying connectivity, with females having higher

403   consistency than males. This may due to the fact that many cognitive process involve higher levels of

404   brain activation in females than males, e.g., empathy for pain (Christov-Moore and Iacoboni, 2019; Groen

405   et al., 2013) and language processing (Burman et al., 2008). But due to the complexity of the movie

406   stimuli, it is difficult to pinpoint a specific cognitive process that solely explains the observed sex

407   differences. Moreover, sex differences may interact with other factors such as age (Etchell et al., 2018).

18

408   We did not explore the interaction effects in the current study due to the limited sample size, but this

409   effect needs to be studied in future works with larger samples.

410   In contrast to our hypothesis, the behavioral prediction analyses showed that only stationary

411   connectivity, but not time-varying connectivity or regional activity, could predict FSIQ scores. Stationary

412   connectivity could reliably predict FSIQ from both the video clips. The contents of the movie clips

413   involve social interactions, which may not be related to general intelligence abilities. Indeed, brain

414   regions that are generally associated with FSIQ are higher-order association regions, such as the lateral

415   prefrontal cortex (Cole et al., 2012; Geake and Hansen, 2005). The prediction features in the current

416   analysis (Figure 5C and 5D) supported this point. Because stationary connectivity remains stable across

417   different conditions, it may reflect general characteristics of cognitive functions, such as FSIQ (Finn and

418   Bandettini, 2021). On the other hand, time-varying connectivity may be sensitive to certain movie

419   contents, therefore not reflecting general cognitive ability. In terms of the SCQ scores, none of the brain

420   measures could predict individual differences in SCQ scores. The SCQ score was chosen because it

421   reflects deficits in social functions related to autism. A study has reported an association between brain

422   activity and SCQ scores at certain time points using the same HBN dataset (Richardson, 2019). With a

423   whole-brain predictive modeling approach with cross-validation, we could not find reliable associations

424   between brain measures and SCQ scores. The association may exist, but be restricted to brain activity

425   during certain events. Alternatively, in this normative sample there may not be a large range of SCQ

426   scores. Therefore, the association between brain measures and SCQ scores in a healthy sample may be

427   weak.

428   The current study analyzed two animated video clips. Many aspects of individual differences

429   appeared to be different between the two clips. For example, the preferred age models and sex effects for

430   both the stationery and time-varying connectivity turned out to be very different between the two clips.

431   This suggests that many of the individual differences depend on the specific movie stimuli. On one hand,

432   this may be desirable, because different movie stimuli may be used to probe different brain functions. On

19

433   the other hand, this means that one should be careful when interpreting results of movie watching studies,

434   as they might be highly sensitive to the stimuli presented.

435

436   **5. Conclusion**

437   In the current study, we examined age and sex effects, and behavioral correlates of time-varying and

438   stationary connectivity during movie watching. We found that time-varying connectivity is more sensitive

439   to the age and sex effects. However, only stationary connectivity could predict individuals' FSIQ scores.

440   These results provide a more detailed portrait of individual differences in time-varying and stationary

441   connectivity in the human brain.

442

443

448

449

450   **Reference:**

451   Abrol, A., Damaraju, E., Miller, R.L., Stephen, J.M., Claus, E.D., Mayer, A.R., Calhoun, V.D., 2017.
452   Replicability of time-varying connectivity patterns in large resting state fMRI samples.
453   NeuroImage 163, 160–176. https://doi.org/10.1016/j.neuroimage.2017.09.020
454   Alexander, L.M., Escalera, J., Ai, L., Andreotti, C., Febre, K., Mangone, A., Vega-Potler, N., Langer, N.,
455   Alexander, A., Kovacs, M., Litke, S., O'Hagan, B., Andersen, J., Bronstein, B., Bui, A., Bushey,
456   M., Butler, H., Castagna, V., Camacho, N., Chan, E., Citera, D., Clucas, J., Cohen, S., Dufek, S.,
457   Eaves, M., Fradera, B., Gardner, J., Grant-Villegas, N., Green, G., Gregory, C., Hart, E., Harris,
458   S., Horton, M., Kahn, D., Kabotyanski, K., Karmel, B., Kelly, S.P., Kleinman, K., Koo, B.,
459   Kramer, E., Lennon, E., Lord, C., Mantello, G., Margolis, A., Merikangas, K.R., Milham, J.,
460   Minniti, G., Neuhaus, R., Levine, A., Osman, Y., Parra, L.C., Pugh, K.R., Racanello, A.,
461   Restrepo, A., Saltzman, T., Septimus, B., Tobe, R., Waltz, R., Williams, A., Yeo, A., Castellanos,
462   F.X., Klein, A., Paus, T., Leventhal, B.L., Craddock, R.C., Koplewicz, H.S., Milham, M.P., 2017.
463   An open resource for transdiagnostic research in pediatric mental health and learning disorders.
464   Scientific Data 4, 1–26. https://doi.org/10.1038/sdata.2017.181

Allen, E.A., Damaraju, E., Plis, S.M., Erhardt, E.B., Eichele, T., Calhoun, V.D., 2014. Tracking whole-brain connectivity dynamics in the resting state. Cerebral cortex (New York, N.Y.: 1991) 24, 663–76. https://doi.org/10.1093/cercor/bhs352

Allen, M., Frank, D., Glen, J.C., Fardo, F., Callaghan, M.F., Rees, G., 2017. Insula and somatosensory cortical myelination and iron markers underlie individual differences in empathy. Sci Rep 7, 43316. https://doi.org/10.1038/srep43316

Ashburner, J., 2007. A fast diffeomorphic image registration algorithm. NeuroImage 38, 95–113. https://doi.org/10.1016/j.neuroimage.2007.07.007

Biswal, B., Yetkin, F.Z., Haughton, V.M., Hyde, J.S., 1995. Functional connectivity in the motor cortex of resting human brain using echo-planar MRI. Magnetic resonance in medicine: official journal of the Society of Magnetic Resonance in Medicine / Society of Magnetic Resonance in Medicine 34, 537–41. https://doi.org/10.1002/mrm.1910340409

Biswal, B.B., Mennes, M., Zuo, X.-N., Gohel, S., Kelly, C., Smith, S.M., Beckmann, C.F., Adelstein, J.S., Buckner, R.L., Colcombe, S., Dogonowski, A.-M., Ernst, M., Fair, D., Hampson, M., Hoptman, M.J., Hyde, J.S., Kiviniemi, V.J., Kötter, R., Li, S.-J., Lin, C.-P., Lowe, M.J., Mackay, C., Madden, D.J., Madsen, K.H., Margulies, D.S., Mayberg, H.S., McMahon, K., Monk, C.S., Mostofsky, S.H., Nagel, B.J., Pekar, J.J., Peltier, S.J., Petersen, S.E., Riedl, V., Rombouts, S.A.R.B., Rypma, B., Schlaggar, B.L., Schmidt, S., Seidler, R.D., Siegle, G.J., Sorg, C., Teng, G.-J., Veijola, J., Villringer, A., Walter, M., Wang, L., Weng, X.-C., Whitfield-Gabrieli, S., Williamson, P., Windischberger, C., Zang, Y.-F., Zhang, H.-Y., Castellanos, F.X., Milham, M.P., 2010. Toward discovery science of human brain function. Proceedings of the National Academy of Sciences of the United States of America 107, 4734–9. https://doi.org/10.1073/pnas.0911855107

Burman, D.D., Bitan, T., Booth, J.R., 2008. Sex differences in neural processing of language among children. Neuropsychologia 46, 1349–1362. https://doi.org/10.1016/j.neuropsychologia.2007.12.021

Calhoun, V.D., Adali, T., Pearlson, G.D., Pekar, J.J., 2001. A method for making group inferences from functional MRI data using independent component analysis. Human brain mapping 14, 140–51.

Cantlon, J.F., Li, R., 2013. Neural Activity during Natural Viewing of Sesame Street Statistically Predicts Test Scores in Early Childhood. PLOS Biology 11, e1001462. https://doi.org/10.1371/journal.pbio.1001462

Christov-Moore, L., Iacoboni, M., 2019. Sex differences in somatomotor representations of others' pain: a permutation-based analysis. Brain Struct Funct 224, 937–947. https://doi.org/10.1007/s00429-018-1814-y

Cohen, S.S., Tottenham, N., Baldassano, C., 2022. Developmental changes in story-evoked responses in the neocortex and hippocampus. eLife 11, e69430. https://doi.org/10.7554/eLife.69430

Cole, M.W., Yarkoni, T., Repovš, G., Anticevic, A., Braver, T.S., 2012. Global Connectivity of Prefrontal Cortex Predicts Cognitive Control and Intelligence. J. Neurosci. 32, 8988–8999. https://doi.org/10.1523/JNEUROSCI.0536-12.2012

Di, X., Biswal, B.B., 2022. Principal component analysis reveals multiple consistent responses to naturalistic stimuli in children and adults. Human Brain Mapping 43, 3332–3345. https://doi.org/10.1002/hbm.25568

Di, X., Biswal, B.B., 2020. Intersubject consistent dynamic connectivity during natural vision revealed by functional MRI. NeuroImage 116698. https://doi.org/10.1016/j.neuroimage.2020.116698

Di, X., Zhang, Z., Xu, T., Biswal, B.B., 2022. Dynamic and stationary brain connectivity during movie watching as revealed by functional MRI. Brain Struct Funct. https://doi.org/10.1007/s00429-022-02522-w

Eichenbaum, A., Pappas, I., Lurie, D., Cohen, J.R., D'Esposito, M., 2021. Differential contributions of static and time-varying functional connectivity to human behavior. Network Neuroscience 5, 145–165. https://doi.org/10.1162/netn_a_00172

21

515   Etchell, A., Adhikari, A., Weinberg, L.S., Choo, A.L., Garnett, E.O., Chow, H.M., Chang, S.-E., 2018. A
516   systematic literature review of sex differences in childhood language and brain development.
517   Neuropsychologia 114, 19–31. https://doi.org/10.1016/j.neuropsychologia.2018.04.011
518   Faghiri, A., Stephen, J.M., Wang, Y.-P., Wilson, T.W., Calhoun, V.D., 2018. Changing brain connectivity
519   dynamics: From early childhood to adulthood. Human Brain Mapping 39, 1108–1117.
520   https://doi.org/10.1002/hbm.23896
521   Faskowitz, J., Esfahlani, F.Z., Jo, Y., Sporns, O., Betzel, R.F., 2020. Edge-centric functional network
522   representations of human cerebral cortex reveal overlapping system-level architecture. Nat
523   Neurosci 23, 1644–1654. https://doi.org/10.1038/s41593-020-00719-y
524   Finn, E.S., Bandettini, P.A., 2021. Movie-watching outperforms rest for functional connectivity-based
525   prediction of behavior. NeuroImage 235, 117963.
526   https://doi.org/10.1016/j.neuroimage.2021.117963
527   Friston, K.J., 1994. Functional and effective connectivity in neuroimaging: A synthesis. Human Brain
528   Mapping 2, 56–78. https://doi.org/10.1002/hbm.460020107
529   Friston, K.J., Williams, S., Howard, R., Frackowiak, R.S., Turner, R., 1996. Movement-related effects in
530   fMRI time-series. Magnetic resonance in medicine : official journal of the Society of Magnetic
531   Resonance in Medicine / Society of Magnetic Resonance in Medicine 35, 346–55.
532   https://doi.org/DOI 10.1002/mrm.1910350312
533   Fu, Z., Tu, Y., Di, X., Du, Y., Sui, J., Biswal, B.B., Zhang, Z., de Lacy, N., Calhoun, V.D., 2019.
534   Transient increased thalamic-sensory connectivity and decreased whole-brain dynamism in
535   autism. NeuroImage 190, 191–204. https://doi.org/10.1016/j.neuroimage.2018.06.003
536   Geake, J.G., Hansen, P.C., 2005. Neural correlates of intelligence as revealed by fMRI of fluid analogies.
537   NeuroImage 26, 555–564. https://doi.org/10.1016/j.neuroimage.2005.01.035
538   Groen, Y., Wijers, A.A., Tucha, O., Althaus, M., 2013. Are there sex differences in ERPs related to
539   processing empathy-evoking pictures? Neuropsychologia 51, 142–155.
540   https://doi.org/10.1016/j.neuropsychologia.2012.11.012
541   Hasson, U., Nir, Y., Levy, I., Fuhrmann, G., Malach, R., 2004. Intersubject synchronization of cortical
542   activity during natural vision. Science (New York, N.Y.) 303, 1634–40.
543   https://doi.org/10.1126/science.1089506
544   Jin, C., Jia, H., Lanka, P., Rangaprakash, D., Li, L., Liu, T., Hu, X., Deshpande, G., 2017. Dynamic brain
545   connectivity is a better predictor of PTSD than static connectivity. Human Brain Mapping 38,
546   4479–4496. https://doi.org/10.1002/hbm.23676
547   Kauppi, J.-P., Jääskeläinen, I.P., Sams, M., Tohka, J., 2010. Inter-subject correlation of brain
548   hemodynamic responses during watching a movie: localization in space and frequency. Front.
549   Neuroinform. 4. https://doi.org/10.3389/fninf.2010.00005
550   Lamm, C., Nusbaum, H.C., Meltzoff, A.N., Decety, J., 2007. What Are You Feeling? Using Functional
551   Magnetic Resonance Imaging to Assess the Modulation of Sensory and Affective Responses
552   during Empathy for Pain. PLOS ONE 2, e1292. https://doi.org/10.1371/journal.pone.0001292
553   Margulies, D.S., Ghosh, S.S., Goulas, A., Falkiewicz, M., Huntenburg, J.M., Langs, G., Bezgin, G.,
554   Eickhoff, S.B., Castellanos, F.X., Petrides, M., Jefferies, E., Smallwood, J., 2016. Situating the
555   default-mode network along a principal gradient of macroscale cortical organization. PNAS 113,
556   12574–12579. https://doi.org/10.1073/pnas.1608282113
557   Marusak, H.A., Calhoun, V.D., Brown, S., Crespo, L.M., Sala-Hamrick, K., Gotlib, I.H., Thomason, M.E.,
558   2017. Dynamic functional connectivity of neurocognitive networks in children. Human Brain
559   Mapping 38, 97–108. https://doi.org/10.1002/hbm.23346
560   Nastase, S.A., Gazzola, V., Hasson, U., Keysers, C., 2019. Measuring shared responses across subjects
561   using intersubject correlation. Soc Cogn Affect Neurosci 14, 667–685.
562   https://doi.org/10.1093/scan/nsz037
563   O'Connor, D., Potler, N.V., Kovacs, M., Xu, T., Ai, L., Pellman, J., Vanderwal, T., Parra, L.C., Cohen, S.,
564   Ghosh, S., Escalera, J., Grant-Villegas, N., Osman, Y., Bui, A., Craddock, R.C., Milham, M.P.,
565   2017. The Healthy Brain Network Serial Scanning Initiative: a resource for evaluating inter-

566   individual differences and their reliabilities across scan conditions and sessions. Gigascience 6,
567   1–14. https://doi.org/10.1093/gigascience/giw011
568 Petroni, A., Cohen, S.S., Ai, L., Langer, N., Henin, S., Vanderwal, T., Milham, M.P., Parra, L.C., 2018.
569   The Variability of Neural Responses to Naturalistic Videos Change with Age and Sex. eNeuro 5.
570   https://doi.org/10.1523/ENEURO.0244-17.2017
571 Portet, S., 2020. A primer on model selection using the Akaike Information Criterion. Infectious Disease
572   Modelling 5, 111–128. https://doi.org/10.1016/j.idm.2019.12.010
573 Rashid, B., Arbabshirani, M.R., Damaraju, E., Cetin, M.S., Miller, R., Pearlson, G.D., Calhoun, V.D.,
574   2016. Classification of schizophrenia and bipolar patients using static and dynamic resting-state
575   fMRI brain connectivity. NeuroImage 134, 645–657.
576   https://doi.org/10.1016/j.neuroimage.2016.04.051
577 Rashid, B., Blanken, L.M.E., Muetzel, R.L., Miller, R., Damaraju, E., Arbabshirani, M.R., Erhardt, E.B.,
578   Verhulst, F.C., van der Lugt, A., Jaddoe, V.W.V., Tiemeier, H., White, T., Calhoun, V., 2018.
579   Connectivity dynamics in typical development and its relationship to autistic traits and autism
580   spectrum disorder. Human Brain Mapping 39, 3127–3142. https://doi.org/10.1002/hbm.24064
581 Richardson, H., 2019. Development of brain networks for social functions: Confirmatory analyses in a
582   large open source dataset. Developmental Cognitive Neuroscience 37, 100598.
583   https://doi.org/10.1016/j.dcn.2018.11.002
584 Rutter, M., Bailey, A., Lord, C., 2003. The social communication questionnaire.
585 Tian, L., Ye, M., Chen, C., Cao, X., Shen, T., 2021. Consistency of functional connectivity across
586   different movies. NeuroImage 233, 117926. https://doi.org/10.1016/j.neuroimage.2021.117926
587 Vanderwal, T., Eilbott, J., Castellanos, F.X., 2019. Movies in the magnet: Naturalistic paradigms in
588   developmental functional neuroimaging. Developmental Cognitive Neuroscience 36, 100600.
589   https://doi.org/10.1016/j.dcn.2018.10.004
590 Vanderwal, T., Eilbott, J., Kelly, C., Frew, S.R., Woodward, T.S., Milham, M.P., Castellanos, F.X., 2021.
591   Stability and similarity of the pediatric connectome as developmental measures. NeuroImage 226,
592   117537. https://doi.org/10.1016/j.neuroimage.2020.117537
593 Vieira, B.H., Pamplona, G.S.P., Fachinello, K., Silva, A.K., Foss, M.P., Salmon, C.E.G., 2022. On the
594   prediction of human intelligence from neuroimaging: A systematic review of methods and
595   reporting. Intelligence 93, 101654. https://doi.org/10.1016/j.intell.2022.101654
596 Wagenmakers, E.-J., Farrell, S., 2004. AIC model selection using Akaike weights. Psychonomic Bulletin
597   & Review 11, 192–196. https://doi.org/10.3758/BF03206482
598 Wechsler, D., 2014. The Wechsler intelligence scale for children—fifth edition.
599 Xia, M., Wang, J., He, Y., 2013. BrainNet Viewer: a network visualization tool for human brain
600   connectomics. PloS one 8, e68910. https://doi.org/10.1371/journal.pone.0068910
601 Yarkoni, T., Poldrack, R.A., Nichols, T.E., Van Essen, D.C., Wager, T.D., 2011. Large-scale automated
602   synthesis of human functional neuroimaging data. Nature methods 8, 665–70.
603   https://doi.org/10.1038/nmeth.1635
604 Yeo, B.T.T., Krienen, F.M., Sepulcre, J., Sabuncu, M.R., Lashkari, D., Hollinshead, M., Roffman, J.L.,
605   Smoller, J.W., Zöllei, L., Polimeni, J.R., Fischl, B., Liu, H., Buckner, R.L., 2011. The
606   organization of the human cerebral cortex estimated by intrinsic functional connectivity. Journal
607   of neurophysiology 106, 1125–65. https://doi.org/10.1152/jn.00338.2011
608
609
610